

Charm baryon semileptonic decays with lattice QCD

Stefan Meinel



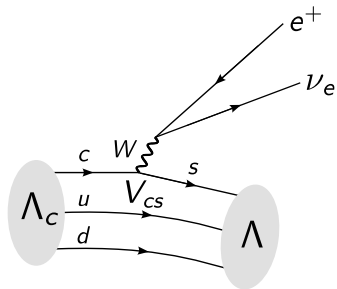
Lattice 2017, Granada

BES III Collaboration, 2015:

First direct measurements of Λ_c branching fractions at $e^+e^- \rightarrow \Lambda_c\bar{\Lambda}_c$ threshold.
Including

$$\mathcal{B}(\Lambda_c \rightarrow \Lambda e^+ \nu_e) = (3.63 \pm 0.38 \pm 0.20)\%$$

[arXiv:1510.02610/PRL 2015]



BES III Collaboration, 2015:

First direct measurements of Λ_c branching fractions at $e^+e^- \rightarrow \Lambda_c \bar{\Lambda}_c$ threshold.
Including

$$\mathcal{B}(\Lambda_c \rightarrow \Lambda e^+ \nu_e) = (3.63 \pm 0.38 \pm 0.20) \% \quad [\text{arXiv:1510.02610/PRL 2015}]$$

From the introduction of their paper:

Since the first observation of the Λ_c^+ baryon in e^+e^- annihilations at the Mark II experiment [4] in 1979, much theoretical effort has been applied towards the study of its SL decay properties. However, predictions of the branching fraction (BF) $\mathcal{B}(\Lambda_c^+ \rightarrow \Lambda e^+ \nu_e)$ in different theoretical models vary in a wide range from 1.4% to 9.2% [5–15], depending on the choice of various Λ_c^+ wave function models and the nature of decay dynamics. In addition, theoretical calculations prove to be quite challenging for lattice quantum chromodynamics (LQCD) due to the complexity of form factors, which describes the hadronic part of the decay dynamics in $\Lambda_c^+ \rightarrow \Lambda e^+ \nu_e$ [16]. Thus, an accurate measurement of $\mathcal{B}(\Lambda_c^+ \rightarrow \Lambda e^+ \nu_e)$ is a key ingredient in calibrating LQCD calculations, which, in turn, will play an important role in understanding different Λ_c^+ SL decays.

- 1 $\Lambda_c \rightarrow \Lambda$ form factors from lattice QCD
[S. Meinel, arXiv:1611.09696/PRL 2016]
- 2 $\Lambda_c \rightarrow p$ form factors from lattice QCD

$$\begin{aligned}
\langle \Lambda(p') | \bar{s} \gamma^\mu c | \Lambda_c(p) \rangle &= \bar{u}_\Lambda \left[(m_{\Lambda_c} - m_\Lambda) \frac{q^\mu}{q^2} f_0 \right. \\
&\quad + \frac{m_{\Lambda_c} + m_\Lambda}{s_+} \left(p^\mu + p'^\mu - (m_{\Lambda_c}^2 - m_\Lambda^2) \frac{q^\mu}{q^2} \right) f_+ \\
&\quad \left. + \left(\gamma^\mu - \frac{2m_\Lambda}{s_+} p^\mu - \frac{2m_{\Lambda_c}}{s_+} p'^\mu \right) f_\perp \right] u_{\Lambda_c},
\end{aligned}$$

$$\begin{aligned}
\langle \Lambda(p') | \bar{s} \gamma^\mu \gamma_5 c | \Lambda_c(p) \rangle &= -\bar{u}_\Lambda \gamma_5 \left[(m_{\Lambda_c} + m_\Lambda) \frac{q^\mu}{q^2} g_0 \right. \\
&\quad + \frac{m_{\Lambda_c} - m_\Lambda}{s_-} \left(p^\mu + p'^\mu - (m_{\Lambda_c}^2 - m_\Lambda^2) \frac{q^\mu}{q^2} \right) g_+ \\
&\quad \left. + \left(\gamma^\mu + \frac{2m_\Lambda}{s_-} p^\mu - \frac{2m_{\Lambda_c}}{s_-} p'^\mu \right) g_\perp \right] u_{\Lambda_c}.
\end{aligned}$$

$$(s_\pm = (m_{\Lambda_c} \pm m_\Lambda)^2 - q^2)$$

- RBC/UKQCD ensembles with $2 + 1$ flavors of domain-wall fermions
[Y. Aoki *et al.*, arXiv:1011.0892/PRD 2011; T. Blum *et al.*, arXiv:1411.7017/PRD 2016]
- Charm action: anisotropic clover
[Z. Brown, W. Detmold, S. Meinel, K. Orginos, arXiv:1409.0497/PRD 2014]
- $c \rightarrow s$ currents: “Mostly nonperturbative” renormalization
[A. El-Khadra *et al.*, hep-ph/0101023/PRD 2001],
one-loop coefficients computed by Christoph Lehner
[C. Lehner, arXiv:1211.4013/PoS 2012]

$N_s^3 \times N_t$	a [fm]	$am_{u,d}$	m_π [MeV]	$am_s^{(\text{val})}$	$m_{\eta_s}^{(\text{val})}$ [MeV]
$48^3 \times 96$	0.1142(15)	0.00078	139(2)	0.0362	693(9)
$24^3 \times 64$	0.1119(17)	0.005	336(5)	0.04	761(12)
$24^3 \times 64$	0.1119(17)	0.005	336(5)	0.03	665(10)
$32^3 \times 64$	0.0849(12)	0.004	295(4)	0.03	747(10)
$32^3 \times 64$	0.0848(17)	0.006	352(7)	0.03	749(14)

(lattice spacings from $\Upsilon(2S)$ - $\Upsilon(1S)$ splitting computed with NRQCD)

$$\mathcal{R}(t, t') = \frac{\begin{array}{c} \text{Diagram 1} \times \text{Diagram 2} \\ \text{Diagram 3} \times \text{Diagram 4} \end{array}}{\text{Diagram 5} \times \text{Diagram 6}}$$

The figure illustrates the definition of $\mathcal{R}(t, t')$ as a ratio of two tensor products of diagrams. Each diagram is enclosed in a double-line chevron shape representing a network boundary. Two vertical dashed lines indicate source and sink positions, with a horizontal arrow below labeled t representing the source-sink separation. Colored arcs represent paths: blue (u), green (d), and red (s). Black arcs represent paths c . A circled cross \otimes marks a current insertion point.

- Top-left diagram:** Source on the left, sink on the right. Paths u (blue), d (green), and c (black) connect source to sink. Path s (red) goes from source to a circled cross \otimes located between the dashed lines, and then to the sink. A horizontal arrow below the dashed lines is labeled t' .
- Top-right diagram:** Source on the left, sink on the right. Paths u (blue), d (green), and s (red) connect source to sink. Path c (black) goes from source to a circled cross \otimes located to the right of the sink, and then to the sink. A horizontal arrow below the dashed lines is labeled $t - t'$.
- Bottom-left diagram:** Source on the left, sink on the right. Paths u (blue), d (green), and c (black) connect source to sink. A horizontal arrow below the dashed lines is labeled t .
- Bottom-right diagram:** Source on the left, sink on the right. Paths u (blue), d (green), and s (red) connect source to sink. A horizontal arrow below the dashed lines is labeled t .

t = source-sink separation
 t' = current insertion time

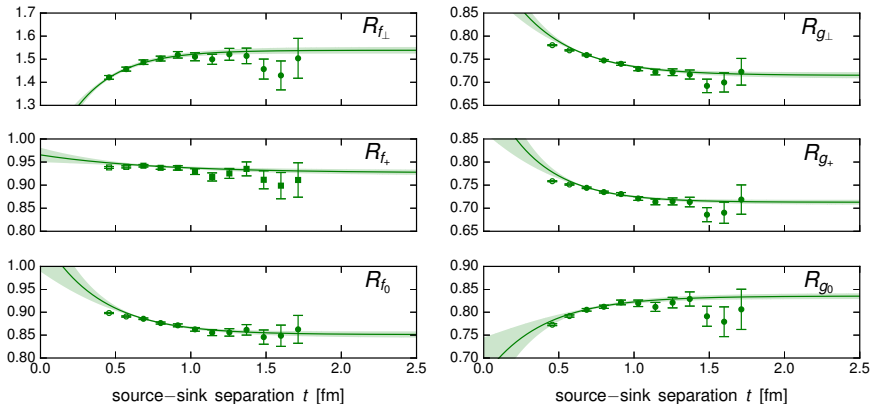
$$R_{f_+}(t) = \frac{2q^2}{(E_\Lambda - m_\Lambda)(m_{\Lambda_c} + m_\Lambda)} \sqrt{\frac{E_\Lambda}{E_\Lambda + m_\Lambda} \mathcal{R}_+^V(t, t/2)} = f_+ + \text{excited state contrib.}$$

$$R_{f_\perp}(t) = \frac{1}{E_\Lambda - m_\Lambda} \sqrt{\frac{E_\Lambda}{E_\Lambda + m_\Lambda} \mathcal{R}_\perp^V(t, t/2)} = f_\perp + \text{excited state contrib.}$$

$$R_{f_0}(t) = \frac{2}{m_{\Lambda_c} - m_\Lambda} \sqrt{\frac{E_\Lambda}{E_\Lambda + m_\Lambda} \mathcal{R}_0^V(t, t/2)} = f_0 + \text{excited state contrib.}$$

(and similarly for g_+ , g_\perp , g_0)

Data from $48^3 \times 96$ lattice, $m_\pi = 139(2)$ MeV, $\mathbf{p}'^2 = 1 (2\pi/L)^2$



The fits are of the form

$$R_f(t) = f + A_f e^{-\delta_f t}$$

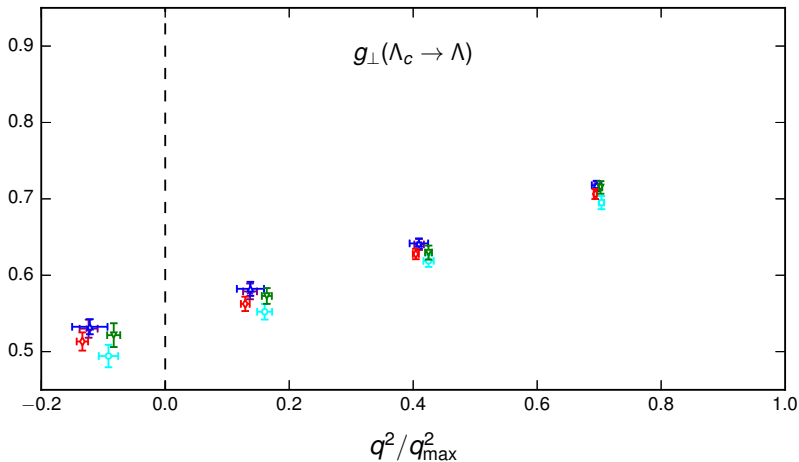
✚ $a = 0.112$ fm, $m_\pi = 336$ MeV, $m_{\eta_s} = 761$ MeV

✚ $a = 0.112$ fm, $m_\pi = 336$ MeV, $m_{\eta_s} = 665$ MeV

✚ $a = 0.114$ fm, $m_\pi = 139$ MeV, $m_{\eta_s} = 693$ MeV

✚ $a = 0.085$ fm, $m_\pi = 352$ MeV, $m_{\eta_s} = 749$ MeV

✚ $a = 0.085$ fm, $m_\pi = 295$ MeV, $m_{\eta_s} = 747$ MeV



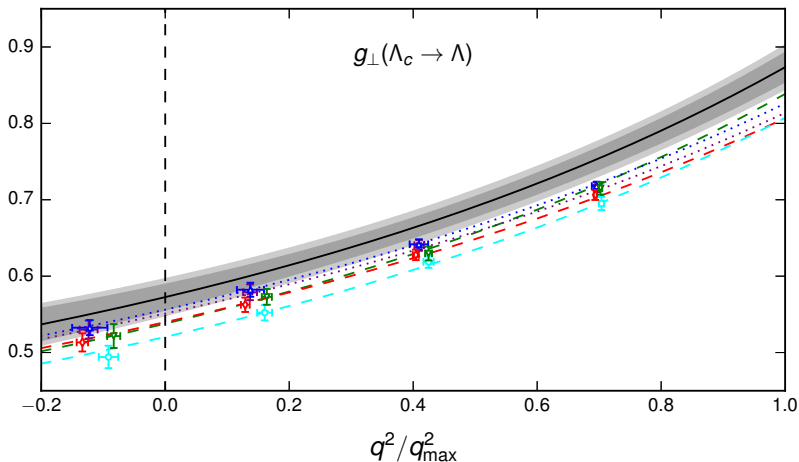
Combined chiral/continuum/kinematic extrapolation using modified z-expansion

[C. Bourrely, I. Caprini, L. Lellouch, arXiv:0807.2722/PRD 2009]

$$z(q^2) = \frac{\sqrt{t_+ - q^2} - \sqrt{t_+ - t_0}}{\sqrt{t_+ - q^2} + \sqrt{t_+ - t_0}}, \quad t_+ = (m_D + m_K)^2, \quad t_0 = (m_{\Lambda_c} - m_\Lambda)^2$$

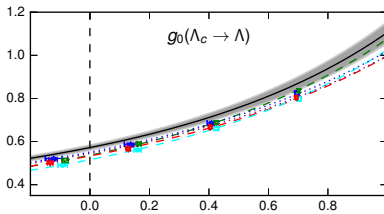
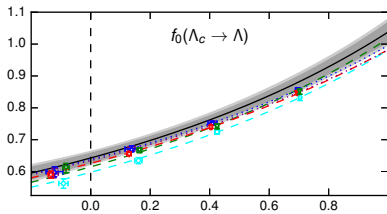
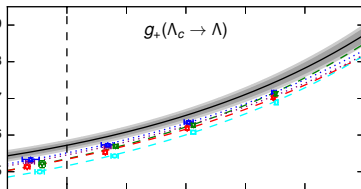
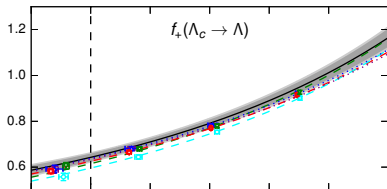
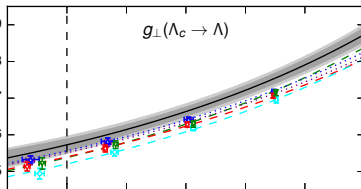
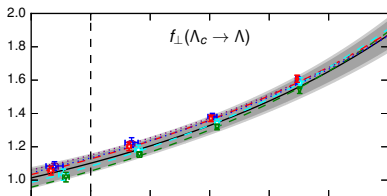
Nominal fit:

$$f(q^2) = \frac{1}{1 - q^2/(m_{\text{pole}}^f)^2} \left[a_0^f \left(1 + c_0^f \frac{m_\pi^2 - m_{\pi,\text{phys}}^2}{\Lambda_\chi^2} + c_{s,0}^f \frac{m_{\eta_s}^2 - m_{\eta_s,\text{phys}}^2}{\Lambda_\chi^2} \right) + a_1^f z(q^2) + a_2^f [z(q^2)]^2 \right] \times \left[1 + b^f a^2 |\mathbf{p}'|^2 + d^f a^2 \Lambda_{\text{QCD}}^2 \right]$$



Inner band: statistical uncertainty from nominal fit only

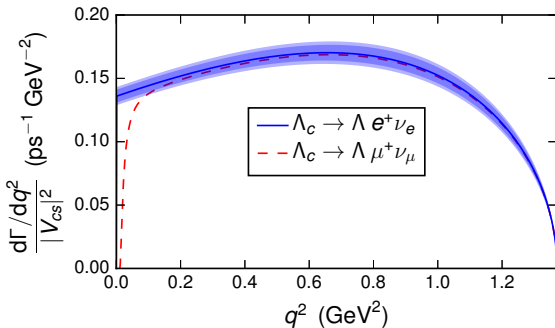
Outer band: includes systematic uncertainty estimated using higher-order fit



q^2/q_{\max}^2

q^2/q_{\max}^2

Predicted differential and total decay rates without $|V_{cs}|^2$:



$$\frac{\Gamma(\Lambda_c \rightarrow \Lambda \ell^+ \nu_\ell)}{|V_{cs}|^2} = \begin{cases} 0.2007(71)(74) \text{ ps}^{-1}, & \ell = e, \\ 0.1945(69)(72) \text{ ps}^{-1}, & \ell = \mu. \end{cases}$$

Taking the indirectly determined $|V_{cs}| = 0.97344(15)$ from UTFit and $\tau_{\Lambda_c} = 0.200(6)$ ps from PDG, the branching fractions predicted by lattice QCD are

$$\mathcal{B}(\Lambda_c \rightarrow \Lambda \ell^+ \nu_\ell) = \begin{cases} 0.0380(19)_{\text{LQCD}(11)\tau_{\Lambda_c}}, & \ell = e, \\ 0.0369(19)_{\text{LQCD}(11)\tau_{\Lambda_c}}, & \ell = \mu. \end{cases}$$

These agree with the BESIII measurements

[arXiv:1510.02610/PRL 2015; arXiv:1611.04382/PLB 2017]

$$\mathcal{B}(\Lambda_c \rightarrow \Lambda \ell^+ \nu_\ell)_{\text{BESIII}} = \begin{cases} 0.0363(43), & \ell = e, \\ 0.0349(53), & \ell = \mu. \end{cases}$$

Alternatively, we can use the lattice QCD results together with the BESIII measurements and τ_{Λ_c} to determine $|V_{cs}|$:

$$|V_{cs}| = 0.949(24)_{\text{LQCD}}(51)_{\text{Exp.}} \quad \text{from } \Lambda_c \rightarrow \Lambda \ell^+ \nu_\ell.$$

For comparison:

$$|V_{cs}| = \begin{cases} 1.008(5)_{\text{LQCD}}(16)_{\text{Exp.}} & \text{from } D_s \rightarrow \ell^+ \nu_\ell \text{ [1, 2]}, \\ 0.975(25)_{\text{LQCD}}(7)_{\text{Exp.}} & \text{from } D \rightarrow K \ell^+ \nu_\ell \text{ [1, 3]}, \\ 0.975(38)_{\text{LQCD}}(4)_{\text{Exp.}} & \text{from } D \rightarrow K \ell^+ \nu_\ell \text{ [4]}, \\ 0.978(35)_{\text{LQCD+Exp.}} & \text{from } D \rightarrow K \ell^+ \nu_\ell \text{ [5]} \end{cases}$$

[1] S. Aoki *et al.* (FLAG), arXiv:1607.00299/EPJC 2017

[2] A. Bazavov *et al.* (Fermilab Lattice and MILC), arXiv:1407.3772/PRD 2014

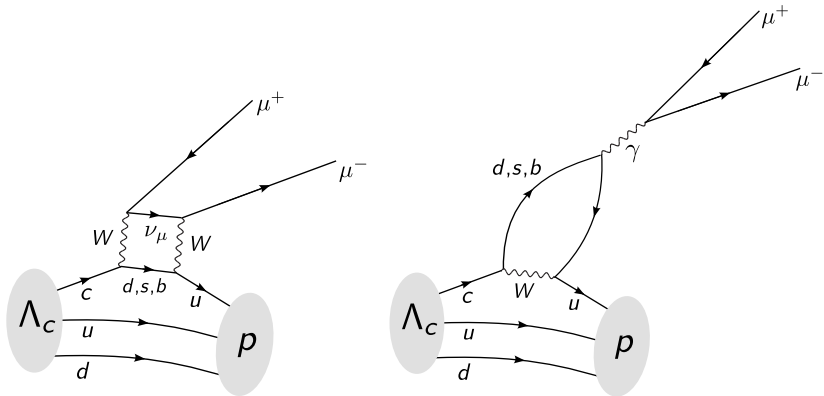
[3] H. Na *et al.* (HPQCD), arXiv:1008.4562/PRD 2010

[4] V. Lubicz *et al.* (ETMC), arXiv:1706.03017

[5] L. Riggio, G. Salerno, S. Simula, arXiv:1706.03657

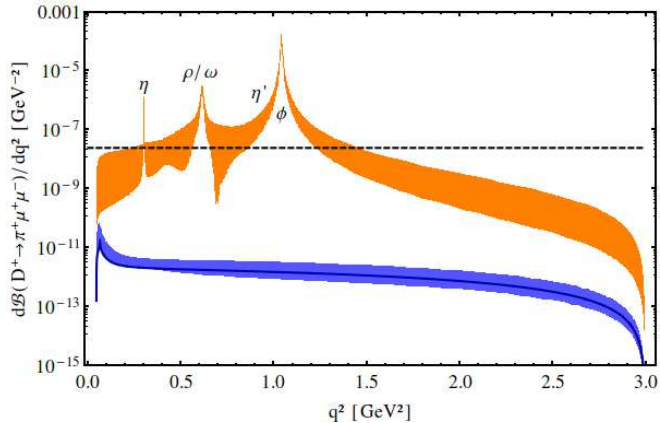
1 $\Lambda_c \rightarrow \Lambda$ form factors from lattice QCD

2 $\Lambda_c \rightarrow p$ form factors from lattice QCD
[preliminary]



Interesting for LHCb!

$c \rightarrow u \mu^+ \mu^-$ decays are dominated by resonant contributions from nonlocal matrix elements.

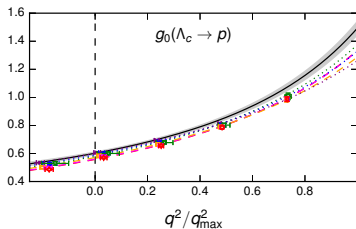
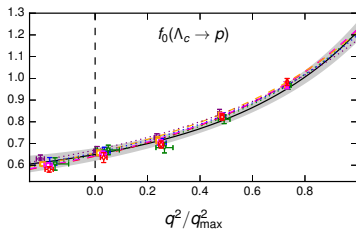
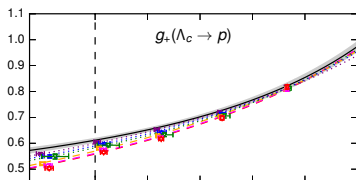
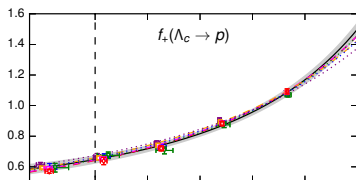
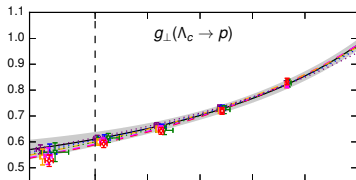
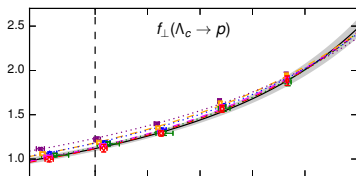


[S. de Boer, G. Hiller, arXiv:1510.00311/PRD 2016]

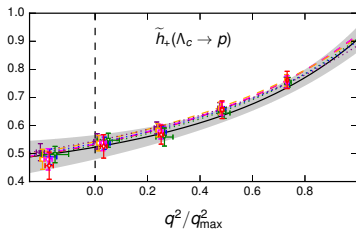
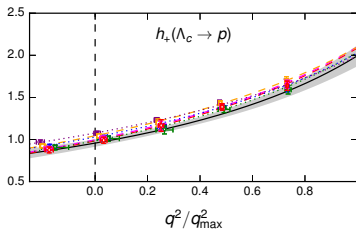
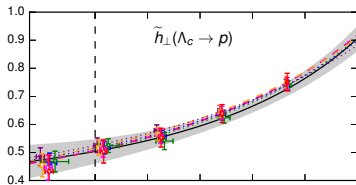
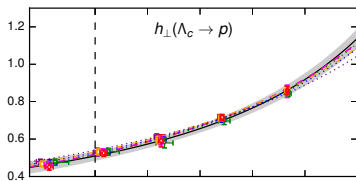
Why are the short-distance $\Lambda_c \rightarrow p$ form factors still useful?

- BSM couplings could be much larger than SM couplings.
Lepton-flavor-violating modes such as $\Lambda_c \rightarrow p e^+ \mu^-$ are short-distance only.
- $\Lambda_c \rightarrow p$ form factors are useful as input for factorization approximation of $\Lambda_c \rightarrow p V(\rightarrow \ell^+ \ell^-)$
- Study m_Q -dependence of $\Lambda_Q \rightarrow p$ form factors
(previous lattice calculations: $m_Q = m_b, m_Q = \infty$)
- Charged-current decay $\Lambda_c \rightarrow n \ell^+ \nu_\ell$

Vector and axial vector form factors – preliminary; only stat. uncertainty shown



Tensor form factors – preliminary; only stat. uncertainty shown



Conclusions and Outlook

- The agreement of the calculated and measured $\Lambda_c \rightarrow \Lambda \ell^+ \nu_\ell$ branching fractions provides a valuable cross-check on the lattice methods, which were previously used for
 - $\Lambda_b \rightarrow p \ell^- \bar{\nu}_\ell$ and $\Lambda_b \rightarrow \Lambda_c \ell^- \bar{\nu}_\ell$
[W. Detmold, C. Lehner, S. Meinel, arXiv:1503.01421/PRD 2015]
 - $\Lambda_b \rightarrow \Lambda \ell^+ \ell^-$
[W. Detmold, S. Meinel, arXiv:1602.01399/PRD 2016]
- The uncertainty in the $|V_{cs}|$ determination from $\Lambda_c \rightarrow \Lambda \ell^+ \nu_\ell$ is currently dominated by the experiments. BESIII will likely take more data at the $\Lambda_c \bar{\Lambda}_c$ threshold in the future.
- The $\Lambda_c \rightarrow p$ form factors will be published soon.
TODO: phenomenology.